LIGHT SOURCE & BEAMLINES

Double RF System for Suppression of Longitudinal Coupled Bunch Instability on the UVSOR Storage Ring

Kazuhiro TAMURA[1], Toshio KASUGA*[1], Makoto TOBIYAMA*[1],
Hiroyuki HAMA[2], Toshio KINOSHITA[2] and Goro ISOYAMA[2]

[1] *Department of Materials Science, Faculty of Science, Hiroshima University, Higashi-Hiroshima 724*

[2] *UVSOR Facility, Institute for Molecular Science, Myodaiji, Okazaki 444*

A higher harmonic RF system whose frequency is the third harmonic of the main RF frequency has been installed on the UVSOR storage ring in order to suppress longitudinal coupled bunch instability with a double RF system. The RF acceleration field with the double RF system is shown in Fig. 1, where the voltage of the third harmonic field is maintained at one third of that of the main RF field. Since the synchrotron oscillation frequency is proportional to the square root of the slope of the RF field and the bunch length is inversely proportional to the synchrotron oscillation frequency, we can control the bunch length by varying the phase of the third harmonic field relative to the main field. Two extreme cases are shown in Figs. 1 (a) and (b). In the (b) mode, the slope of the combined field is twice as much as that of the main RF field alone so that the bunch length is expected to decrease to 70 % of the normal value. In the (a) mode, slopes of the respective field components cancel out, so that not only the bunch length becomes longer but also the frequency spread of the synchrotron oscillation increases due to the non-linearity of the RF field at the electron bunch. The frequency spread leads to Landau damping against the coherent oscillation of electron bunches due to the longitudinal instability.

First, we measured the synchrotron oscillation frequency, the frequency spread and the bunch length in single bunch operation at an electron energy of 600 MeV, in order to see whether the double RF system worked as expected. The main RF system was operated in the same conditions as usual; the frequency is 90.115 MHz, the peak

RF voltage is 47 kV and the tuning angle is around -30 degrees. The resonant frequency of the harmonic cavity ω_{res} was set to be lower than the driving frequency ω. The tuning angle of the cavity Φ defined as

$$\tan\Phi = -\frac{2Q_0}{1+\beta}\left(\frac{\omega-\omega_{res}}{\omega_{res}}\right) \qquad (1)$$

was set at -60 degrees in order to avoid Robinson instability, where Q_0 is the unloaded Q factor, β the coupling coefficient. The bunch length and the synchrotron oscillation frequency were measured in the (a) and (b) modes as a function of the RF voltage of the harmonic cavity. The measured values agreed well with theoretical predictions for the double RF system. Next, we carried out experiments in multi-bunch operation to suppress longitudinal coupled bunch instability. The peak RF voltage in the harmonic cavity was set at 15.6 kV, which is one third of the voltage in the main cavity, and the phase was adjusted to operate the system in the (a) mode. When the beam current was low, the instability was completely suppressed with the double RF system. As the beam current increased, however, it became difficult to keep the phase of the harmonic field due to the beam-induced RF field in the harmonic cavity, and the instability appeared again. Meanwhile, it turned out that the instability could be suppressed even at the higher beam current if the tuning angle of the harmonic cavity was set at a positive value. This result indicates that the strong instability excited by the fundamental resonance of the harmonic cavity can be suppressed by Landau damping with the double RF system. Since the beam induced field in the harmonic cavity at the negative tuning angle is in the same phase as the RF field in the (a) mode, this operation mode works even at a very high beam current.

The double RF system is routinely used for user experiments in multi-bunch operation to suppress longitudinal coupled bunch instability. Another advantage of this system is that the beam lifetime becomes longer because the bunch is 2 ~ 3 times longer. The lifetime at the beam current of 200 mA increases from 240 min to 350 min. The maximum beam current in multi-bunch operation had been limited by the

instability to approximately 500 mA. With the double RF system, it could be increased to more than 1 A.

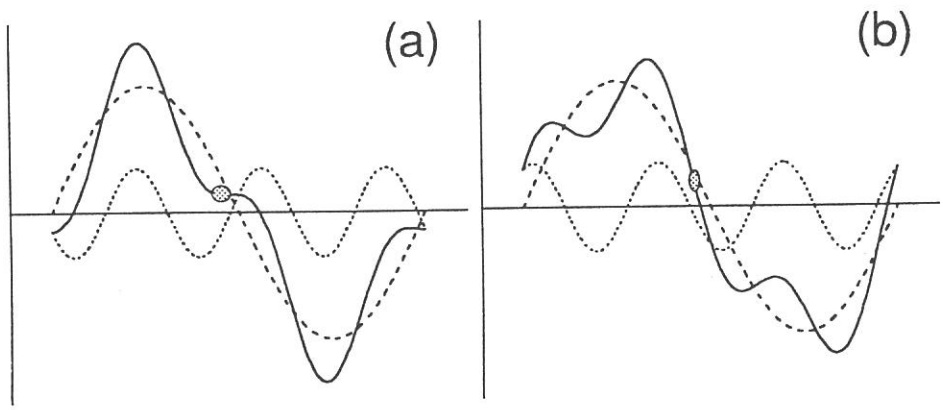

Figure 1. RF field in the double RF system. The peak voltage of the third harmonic field (dotted line) is one third of the main RF field (broken line). The solid line is the combined field. In the (a) mode, the phase of the higher harmonic field is adjusted such that the slope of the combined field becomes zero at the bunch position. In the (b) mode, the slope becomes higher and the bunch length is reduced.

Lasing of a Free Electron Laser in Ultraviolet Region on the UVSOR Storage Ring

Hiroyuki Hama, J. Yamazaki and G. Isoyama
UVSOR Facility, Institute for Molecular Science, Myodaiji, Okazaki 444

We have been carrying out free electron laser (FEL) experiments on the UVSOR storage ring. The first lasing was obtained at wavelengths around 460 nm in Spring, 1992 [1]. Since then, we have been preparing for experiments in the ultraviolet (UV) region. Because the FEL gain and the reflectivity of mirrors used for the optical cavity are anticipated to decrease as the wavelength becomes shorter, we have developed a gain-enhancement technique using a higher harmonic RF cavity (HCV) [2].

The FEL gain is directly proportional to peak density of electrons n_{peak} which is inversely proportional to the bunch length. The bunch length of the UVSOR storage ring can be controlled with a double RF system, which was recently commissioned. When the phase of the RF field in the HCV to that of the main cavity (MCV) is adjusted to make the slope of the RF field steeper, the bunch is shortened and the peak current becomes higher. In this operation mode, the gain is increased independently of the other parameters. For experiments in the UV region, we have kept the electron energy at 500 MeV. We measured the bunch length σ_l with a streak camera at a very low current of less than 0.1 mA. As shown in Fig. 1, the minimum σ_l was 57 ps when the rf voltage in the HCV was set at the maximum value and the phase of the third harmonic field was optimized. On the other hand, regular value of σ_l with the MCV alone is 100 ps. The bunch length with the HCV remains much shorter than that in the regular operation even at higher beam currents. It can be concluded that the gain with the HCV is increased to be approximately 1.7 times higher over the whole range of the wavelength and the beam current.

At first, we chose the wavelength around 340 nm for experiments in the UV

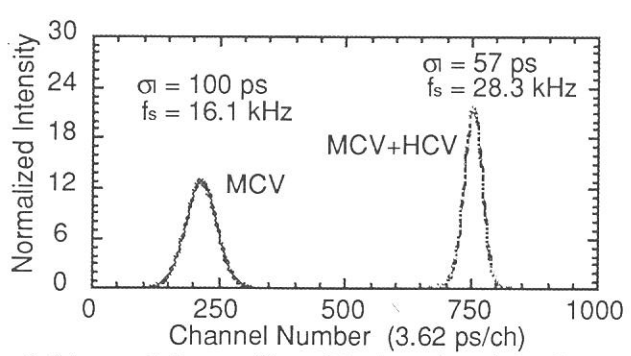

Fig. 1 Measured time profiles of the beam bunch for the normal operation (left) and the operation with the HCV (right).

region. The coating materials of mirrors for 340 nm were same as those used in the visible region. However, it turned out that the mirror degradation was much more serious than in the visible region. The reflectivity of mirrors for 340 nm decreased very much in the longer wavelength side, while that of the mirrors for 490 nm decreased appreciably in the shorter wavelength side. We have not identified exactly the origin of the mirror degradation at present. However, it seems that an absorption band appeared on the region from 340 to 440 nm by irradiation with higher harmonic radiation from the optical klystron. Based on this experience we decided to choose the wavelength at 300 nm for the experiment, where the mirror degradation is less serious. We obtained the first lasing in the UV region at 303 nm on July 5, 1993 with the initial beam current of 22 mA/bunch. The laser wavelength could be varied from 310 nm to 290 nm by changing the undulator gap. As the dose increased, the relative peak intensities at longer wavelengths decreased due to the mirror degradation. The mirror degradation was still serious in the wavelength region above 300 nm. Lasing at 293 nm, where the mirror degradation was less significant, continued until the beam current decayed down to 8.6 mA/bunch. The round-trip reflectivity of mirrors was measured after the lasing experiment to be 99.4 %. The estimated threshold current from the gain and the mirror reflectivity is approximately 9 mA/bunch, which agrees very well with the experimental value.

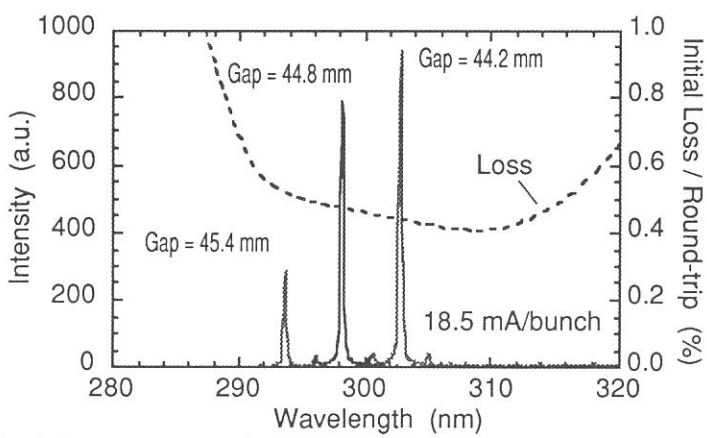

Fig. 2 Laser spectra at the wavelength around 300 nm measured by a monochrometor for various undulator gaps. The initial round-trip loss is also indicated by the dashed line.

We have also conducted experiments to derive the effective gain at the visible region around 500 nm with the gain enhacement technique. The effective gain can be deduced from the time dependent variation of the laser intensity as $G = (I_2 / I_1)^{\frac{1}{n}}$, where I_1 is the intensity at certain time and I_2 is that after n round-trips. Therefore we derived the effective gain as a function of time from the measured shape of the macropulse. In order to secure enough time for beam cooling by radiation damping, lasing was controlled by the gain-switching (G-switching) with a repetition rate of 1

Hz, in which the RF frequency was shifted by 200 Hz to stop lasing. The macropulse was measured with a biplanar photodiode. Time spectra of the laser power were taken by a digital oscilloscope and the data were transferred to a personal computer. Figure 3 shows the experimental value of gain at 490 nm as a function of the beam current, which was derived from the beginning of macropulses in the G-switching mode. The experimental gain is in good agreement with the calculated gain curve with the HCV. It was confirmed that the gain was enhanced as expected by the reduction of the bunch length using the HCV.

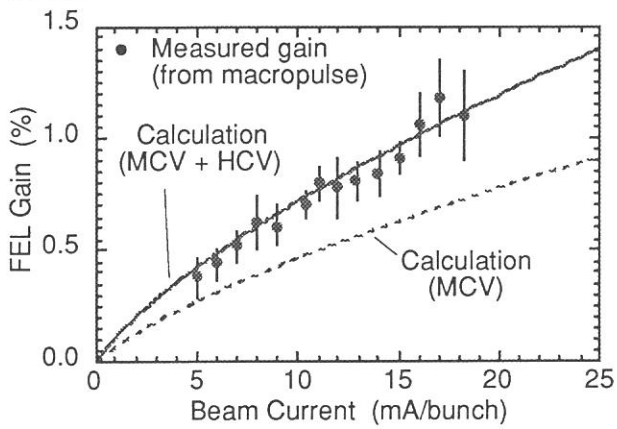

Fig. 3 Beam current dependence of the measured gain derived from the macropulse (solid circle) and the calculated one (solid line). The calculated gain for the normal operation with MCV only is also shown by the dashed line.

The further study including the bunch length measurement during the laser oscillation is in progress.

References

[1] S. Takano, H. Hama and G. Isoyama, Nucl. Instr. and Meth. A331 (1993) 20.

[2] K. Tamura, T. Kasuga, T. Tobiyama, H. Hama, T. Kinoshita and G. Isoyama, submitted to Jpn. J. Appl. Phys.

Improvement of Open Beam Lines

Masao Kamada, Atsunari Hiraya, Shin-ichiro Tanaka, Kusuo Sakai, Osamu Matsudo, Toshio Kinoshita, Jun-ichiro Yamazaki, Eiken Nakamura, and Makoto Watanabe*

UVSOR Facility, Institute for Molecular Science, Myodaiji, Okazaki 444
*Research Institute for Scientific Measurements, Tohoku University, Sendai 980

In 1993, we have carried out improvement of several beam lines opened for outside users as follows.

(1) **BL1B**: In April the device exchanging three gratings for 1-m Seya-Namioka type monochromator was suddenly broken. This is due to the fatigue of supporting springs, and so we repaired it by replacing with new springs. Moreover, when we fixed this trouble, we also replaced the G1 and G3 gratings with new ones, which have 2400 and 600 grooves/mm, respectively. The typical photon flux is now about $1x10^{10}$ photons/s/100mA at 280 nm with 0.1-0.1 mm slits.

(2) **BL2B1**: In March the M0 mirror in the premirror chamber was replaced with new one, since the old one has been used for 7 years. The intensity around 500 eV became ten times intense more than the previous one, but there is still a deep dip around 280 eV, which is due to the C K absorption of contaminated carbon on the mirrors and grating in the Grasshopper monochromator.

(3) **BL3A2**: In October the grating G1 of 2400 grooves/mm was replaced by new one. Then, the available maximum photon energy from the 2.2 m Constant Deviation Grazing Incidence Monochromator was extended up to 125 eV. In December the electronic circuit driving the monochromator was shut down. We doubted the virus coming from outside, but the reason of this trouble was the loosening of the contact of the cable between the linear encoder to ADC.

(4) **BL6A1**: In recent years, the Martin-Pupplet

interferrometer lost the accuracy so often that the users had to measure several times to get reproducibility of the spectra. This is because the thread of a driving gear of a movable mirror has been consumed. Can you imagine how many the mirror in the interferrometer has moved for 8 years ? We guess it is more than 100,000 motions. Thus, the driving mechanism of the interferrogram was replaced with newly constructed one in June. The present performance of the interferrometer is the same as that obtained in 8 years before.

(5) **BL7A**: The motion of the crystals in the double crystal monochromator follows the L-shaped bases moving along the linear guides. This allows us to get monochromatized lights in fixed direction. However, the previous linear guides were so short that the L-shaped bases were tilted slightly at low Bragg angle. In October the linear guides were replaced with new sound and long guides.

(6) **BL7B**: In December the device exchanging three gratings in 1-m Seya-Namioka type monochromator was repaired, since the extraordinary sound happened several times last autumn. This is due to the lack of lubricating powder MoS_2 in the translating and rotating part of the device exchanging and rotating gratings. We also replaced grating G2 and G3 with new ones and got the considerable increase in intensity around 100 nm. The driving mechanism of 1-m Seya-Namioka at BL 7B is not the same as that at BL 1B, but the fact that the driving mechanisms of BL 1B and BL 7B were shut down at almost the same time indicates that it is the good time to consider the renewal of the mechanism of 10-years-old monochromators.

The authors would like to express their sincere thanks to Mrs. N. Mizutani, K. Suzui, and T. Horigome of the machine shop of IMS for their supports and kind advice.

Construction of 15-m Constant-Deviation Grazing Incidence Monochromator with Laminar-type Gratings at BL8B1

Atsunari HIRAYA, Eiken NAKAMURA, Masami HASUMOTO, Toshio KINOSITA, Kusuo SAKAI, Eiji ISHIGURO*, and Makoto WATANABE**

Institute for Molecular Science, Myodaiji, Okazaki 444
**Department of Applied Physics, Osaka City University, Sumiyoshi-ku, Osaka 558*
***Research Institute for Scientific Measurements, Tohoku University, Sendai 980*

A 15-m constant-deviation grazing incidence monochromator was constructed at beamline 8B1. The principle of the monochromator is essentially the same with the monochromator at BL3A2, that is the sum of incident angle and diffraction angle is kept constant (constant deviation) and both entrance and exit slit are fixed (constant length). This monochromator was designed to cover the photon energy 31-620 eV (40.5 - 2 nm) by changing three laminar-type gratings. All gratings are original grating fabricated on synthetic quarts and coated with Au. Parameters of gratings are listed below.

	radius	groove density	lower limit	resolution*	duty factor+	depth	Au-coating
G1	15m	1080/mm	368 eV	92 meV	40%	15 nm	20 nm
G2	15m	540/mm	184 eV	46 meV	35%	20 nm	30 nm
G3	7.5m	360/mm	31 eV	8 meV	40%	20 nm	30 nm

*at lower energy limit, with 10μm slit, +pattern width / groove width

Other parameters of the monochromator and its optical elements are listed below.

acceptance angle	vertical: 1.5mrad, horizontal: 10mrad
M0 (horizontal focus)	spherical mirror: r=86.8m, incidence angle=87.5°
M1 (vertical focus)	bent elliptic mirror: incidence angle 88.5°, L1=6717mm, L2=1680mm, demagnification 1/4
M2	plane mirror
M3	troidal mirror: $r_{vert.}$= 35655mm, $r_{hor.}$ = 86.5mm
Spot size at sample	horizontal: 2.0mm, vertical: 0.7mm

Fig. 1. shows the side view of the monochromator including premirror chamber (M1) and postmirror (M3) chamber. Total electron yield spectrum of TiO_2 obtained with using 1080 *l*/mm (G1) grating is shown in Fig. 2. Monochromatized photons were observed from 360 eV up to about 1 keV. After the final adjustment, this beamline will be used for absorption and total electron yield measurements on gases and solids, as well as fluorescence and (fragment) ion measurements on molecules.

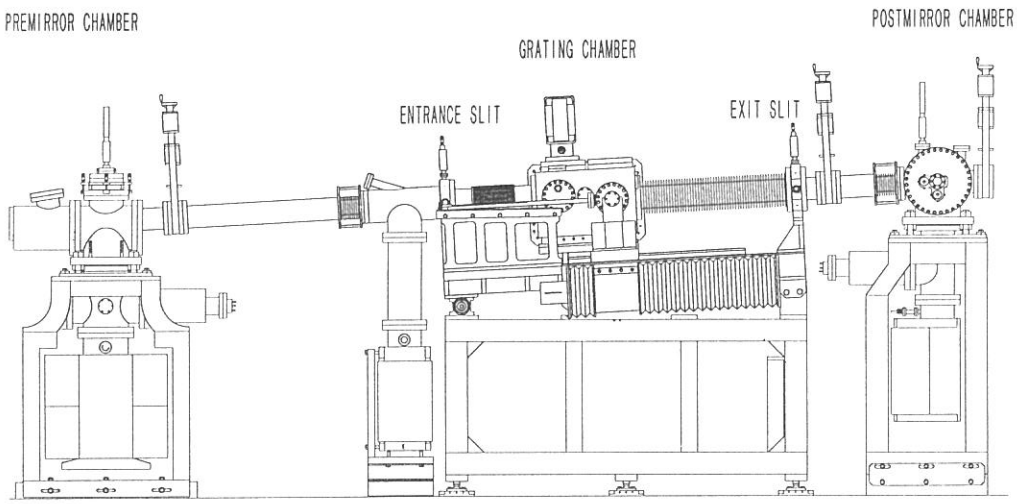

Figure 1. Side view of the monochromator including the premirror and postmirror chambers.

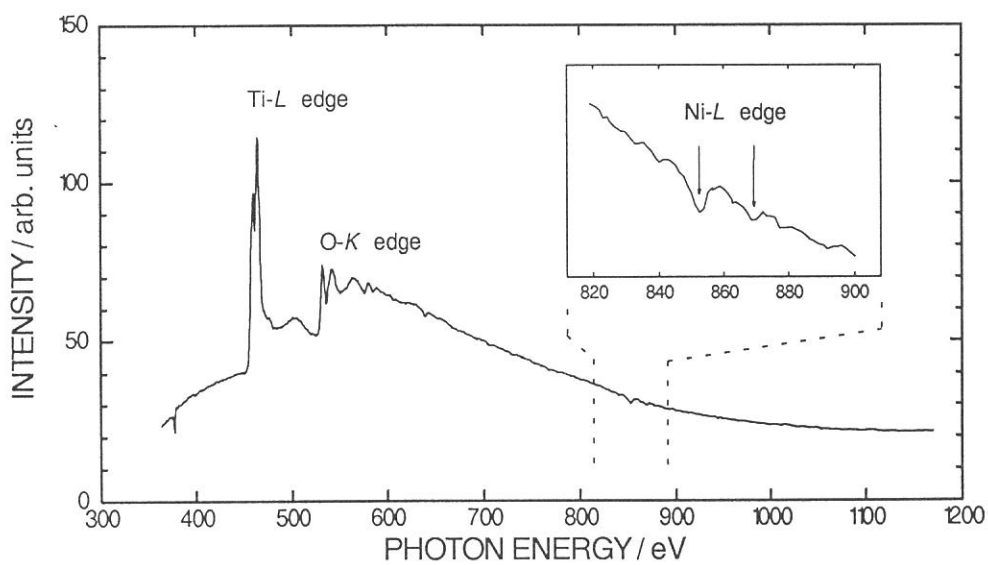

Figure 2. Electron yield spectrum of TiO_2 obtained with 1080 *l*/mm grating (G1).

Development of an Intense Source of Metal-Cluster Anions

Minoru KANNO[†] and Koichiro MITSUKE[§†]

The Graduate University for Advanced Studies,[†] and Institute for Molecular Science,[§]
Myodaiji, Okazaki 444

Study of photodetachment spectroscopy of metal cluster anions is very useful to obtain valuable information on the ground and electronically excited states of neutral clusters. We are constructing a source of metal cluster anions using plasma sputtering. This source is a cluster-ion version of the "BLAKE V" ion source which has been developed by Mori *et al.*[1] to generate intense beam of heavy-mass negative metal ions such as Au^- and Cu^- at National Laboratory for High Energy Physics (KEK) in cooperation with a research group of Tsukuba University.

A photographic view and a schematic diagram of the apparatus are shown in Figs. 1 and 2, respectively. Negative ions are produced at the surface of the sample metal which is placed in a Xe plasma confined by a multicusp magnetic field. The sputtered atomic ions are decelerated by collisions with flowing He gas, and then cluster ions condensed out of the quenched vapor. Atomic and cluster ions extracted from the source are mass-separated by a magnetic mass spectrometer and allowed to intersect at 90° with the dispersed light from a 1 m Seya-Namioka monochromator. The extraction voltage is set to 10 - 20 kV. In the first stage, we are planning to measure threshold photoelectron spectra of size-selected metal cluster anions.

1) Y.Mori, Rev. Sci. Instrum., **63**, 2357 (1992).

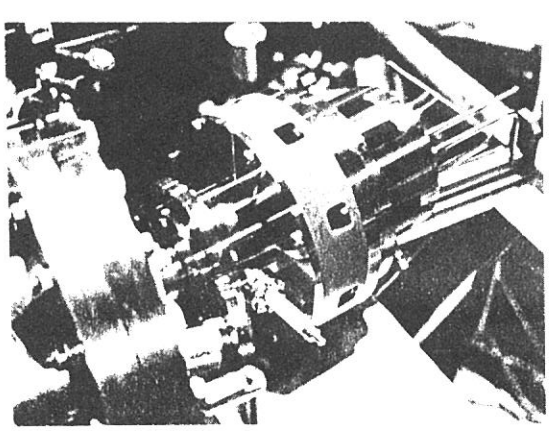

Figure 1. Photographic view of a source of metal-cluster anions.

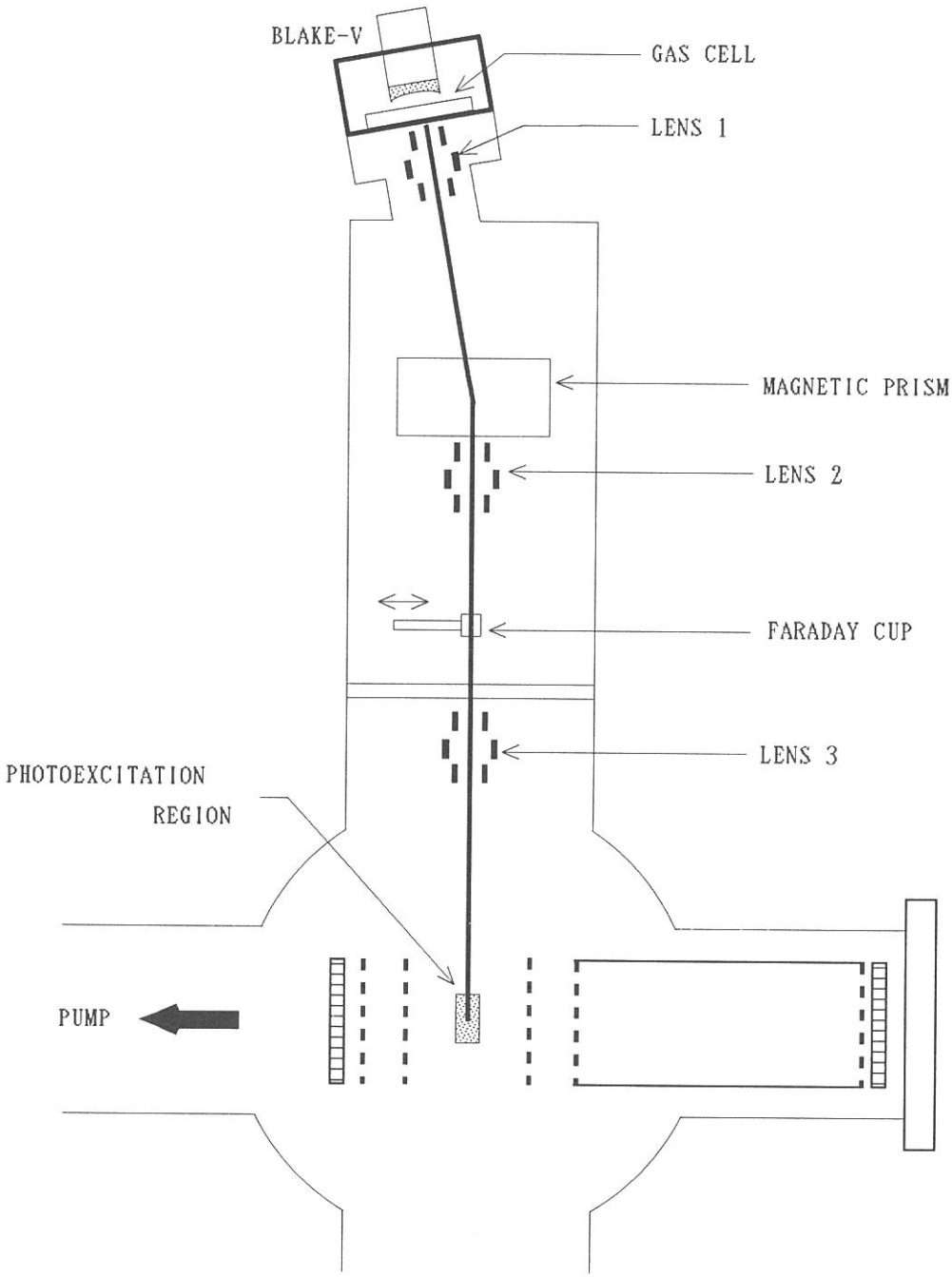

Figure 2. Schematic diagram of the apparatus for photodetachment spectroscopy of metal-cluster anions.

DEVELOPMENT OF HIGH INTENSITY CLUSTER BEAM SOURCE USING A CRYOPUMPING SYSTEM FOR PHOTOIONIZATION AND PHOTODISSOCIATION STUDIES

Hiroaki YOSHIDA and Koichiro MITSUKE

Department of Vacuum UV Photoscience, Institute for Molecular Science, Myodaiji, Okazaki 444

Photoionization and photodissociation studies of atomic or molecular clusters are very important to bridge the gap between atoms or molecules and solids. A great deal of efforts have been made to determine the geometrical structure and ionization potential of clusters. However, dynamical behaviors of clusters excited above their lowest ionization potential are hardly elucidated yet. In such an energy region, superexcitation and decay such as autoionization, neutral dissociation, and ion–pair formation are important in competition with direct ionization. We have been studying the ion–pair formation via molecular superexcited states by a positive ion–negative ion coincidence spectroscopy.[1,2] In order to apply this methodology to investigation of superexcited states of clusters, we have developed a supersonic cluster beam source using a cryopumping system.

A schematic diagram of the apparatus is shown in Fig.1. This type of beam source was originally developed by Hirayama et al. for electron energy loss spectroscopy of rare–gas clusters.[3] The three–stage cryogenic differential pumping system consists of inner and outer cylinders and two stainless steel pipes blazed around each cylinder. The system is mounted on a beam source chamber. A sample gas is expanded into the first stage from a conical nozzle of 100–μm diameter at room temperature (Laser technics, Inc.). A molecular beam is introduced through a conical skimmer with an entrance hole of 380–μm diameter (Beam Dynamics, Inc.) into the second stage and collimated by two slits of 2–mm diameter. The inner and outer cylinders are cooled by cold He and N_2 gases, respectively, flowing through the blazed pipes. The temperature of the wall of the inner cylinder is kept at about 30K. We are now examining the performance of the apparatus.

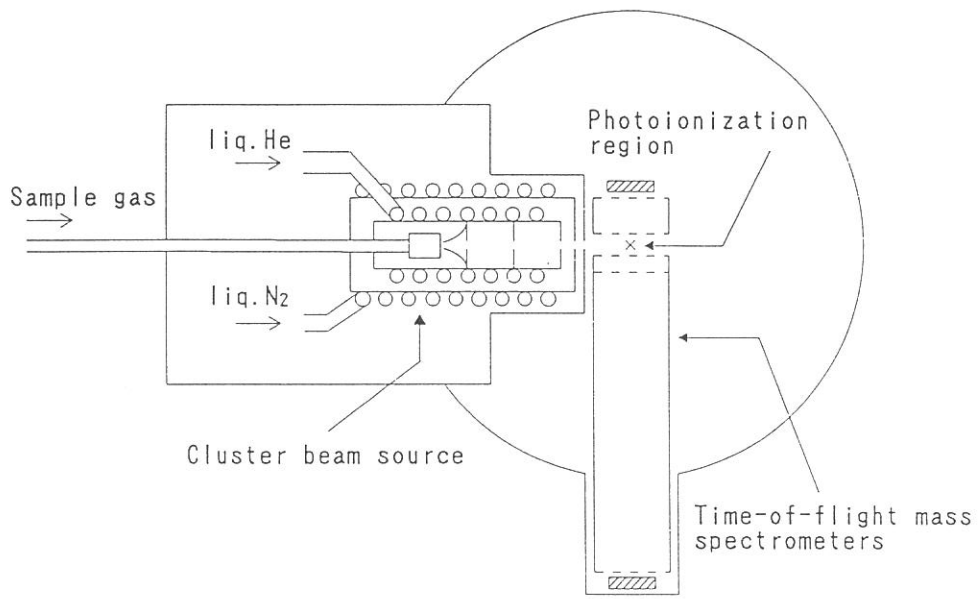

Fig.1 Schematic diagram of the supersonic cluster beam source using a three-stage cryogenic differential pumping system.

References

1) K.Mitsuke, H.Yoshida, and H.Hattori, Z.Phys.D **27**, 267(1993).

2) H.Yoshida and K.Mitsuke, J.Chem.Phys., submitted.

3) T.Hirayama, A.Kanehira, and I.Arakawa, Rev.Sci.Instrum. **64**, 962(1993).

Construction and performance of an apparatus for photoelectron spectroscopy and electron-ion coincidence measurement

Hideo Hattori and Koichiro Mitsuke

Department of Vacuum UV Photoscience, Institute for Molecular Science, Myodaiji, Okazaki 444

Ionization is a major phenomenon for photoexcited molecules in the VUV region. Photoionization cross section curves frequently show characteristic features, associated with a variety of ionization mechanisms.

In attempt to study the ionization mechanism in detail, we have constructed a versatile photoionization spectrometer at the beamline BL3B, as shown in Figure 1. We can make the experiments of photoionization mass spectrometry, photoelectron spectroscopy, constant-ionic-state spectroscopy, and photoelectron-photoion coincidence spectroscopy. This apparatus consists of an electron energy analyzer and a time-of-flight mass spectrometer. The energy analyzer is a 160° spherical electrostatic deflection type. The mean radius of the electron orbit is 54.7 mm. The mass spectrometer containing four grids and a drift tube of 50-cm length, is designed to satisfy space focusing conditions.[1] Measurements and data acquisition are controlled by the CAMAC and NIM system. The molecular beam of a sample gas is expanded into the ionization region from a nozzle of 50-μm diameter, and intersects perpendicularly with a VUV photon beam dispersed by a 3-m normal incidence monochromator. Produced ions are pushed away into the drift tube by a 1kV pulsed electric field and mass-analyzed. On the other hand, ejected electrons are focused onto the entrance slit of the energy analyzer and deflected electrostatically to a different region in space for different kinetic energies. The resolution of the analyzer is estimated to be about 50 meV with photoexcitation at 600 Å.

Figures 2 and 3 show photoelectron spectra of O_2 taken at 584 Å and 885-890 Å, respectively. In Figure 3, a long series of peaks can be seen on the lower energy side of the ionization limit for O_2^+ ($\tilde{X}^2\Pi_g$). The corresponding vibrationally excited states exist in the region of a so-called Franck-Condon gap, and are considered to result from autoionization of Rydberg states converging to upper ionic states. The spectrum at 885 Å shows an irregularly strong intensity of the $v'=5$ component. This may be ascribed to a

large overlap of vibrational wave functions between $O_2^+(\tilde{X}^2\Pi_g, v'=5)$ and the $(3s\sigma_g\,^3\Pi_u, v'=7)$ Rydberg state converging to $O_2^+(\tilde{A}^2\Pi_u)$.

1) W.C.Wiley and I.H.McLaren, Rev. Sci. Instrum. **26**, 1150 (1955).

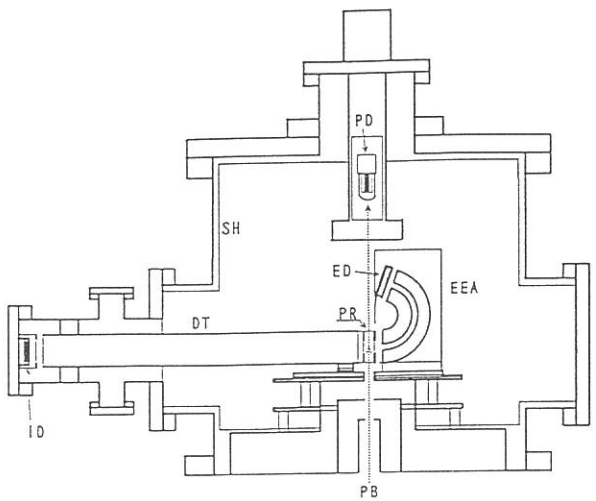

Figure 1. Schematic diagram of the photoionization spectrometer. PB: monochromatized photon beam, PR: photoionization region, DT: drift tube for ions, EEA: electron energy analyzer, ID: ion detector, ED: electron detector, PD: photon detector, SH: μ-metal shield. The molecular beam is introduced into PR perpendicularly to both PB and the symmetric axis of DT.

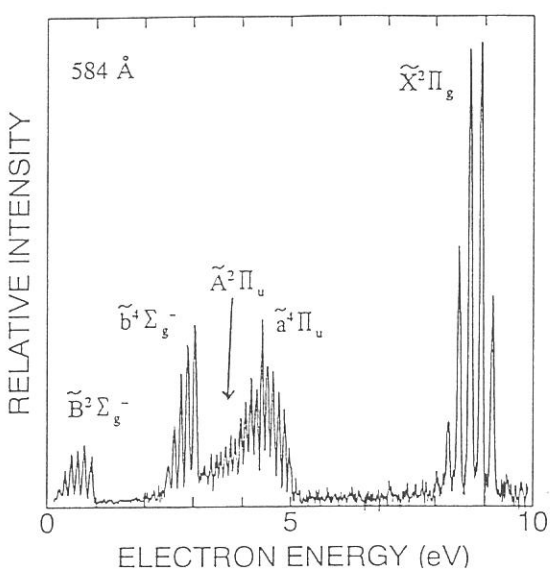

Figure 2. Photoelectron spectrum of O_2 taken with a excitation wavelength of 584 Å.

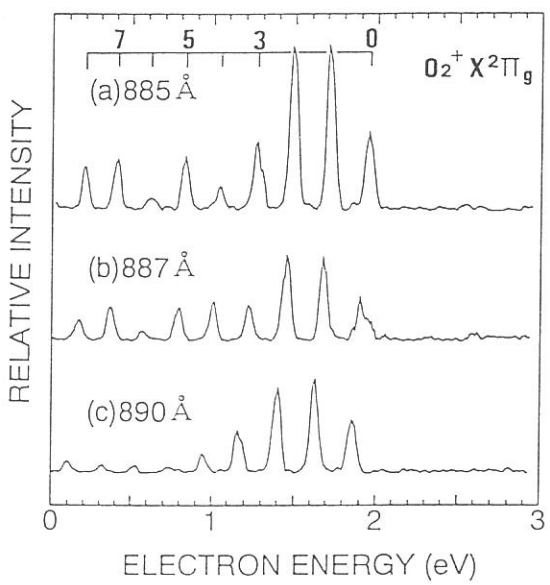

Figure 3. Photoelectron spectra of O_2 taken with excitation wavelengths of (a)885 Å, (b)887 Å and (c)890 Å. The observed band results from a transition to the $\tilde{X}$ ionic state.

CONSTRUCTION OF DEPOSITION SYSTEM IN BEAM LINE BL-4A AND EPITAXIAL GROWTH OF ZnTe BY SYNCHROTRON RADIATION

Mitsuhiro NISHIO, Toshihiro OGATA*, Makoto IKEJIRI* and Gheyas Syed IRFAN*

Institute for Molecular Science, Myodaiji, Okazaki 444, Japan

*Department of Electronic Engineering, Faculty of Science and Engineering, Saga University, Honjo-1, Saga 840, Japan

Low temperature growth is one of the key factors for growing ZnTe of high quality. We have already demonstrated by the experiment in the BL-8A that synchrotron radiation (SR) provides a powerful light source for a novel low-temperature growth technique of ZnTe. In order to investigate systematically the growth of ZnTe, we have constructed the deposition system connected to the analysis chamber in the BL-4A, as shown schematically in fig. 1. Here, the differential pumping system has been designed carefully in order to make sure that the growth experiment can be carried out at a pressure of 10^{-4} Torr without contaminating in the analysis chamber by source gases. Three apertures, each having an inner diameter 8 mm, were used. The length of the aperture near the growth chamber was prepared as long as 350 mm to reduce the conductance and its alignment could be done easily by using the X-Y stages, as shown in the figure.

In this experiment, diethylzinc and diethyltelluride were employed as source materials. Hydrogen was used as a carrier gas. The substrate was (100) oriented GaAs. The growth was carried out at room temperature by two different methods. One is the growth by the repetition of the cycle which is composed of the formation of adsorbed layer of the reactants followed by the irradiation of SR to the resulting layer. Another is the growth in a continuous gas flow in order to investigate the possibility of rapid epitaxial growth. In both cases, the film, having a relatively smooth and featureless surface morphology, was deposited on the substrate. The film was identified as ZnTe epitaxial layer by XPS, X-ray diffraction and RHEED techniques. Furthermore, it should be emphasized that no signals with regard to carbon and oxygen can be detected in the film by XPS and photoluminescence techniques. Figure 2 shows the relationship between the growth thickness and growth cycle in

the former procedure. The growth rate can be estimated to be 6 Å/growth cycle, indicating that the growth thickness can be controlled on an atomic scale by this method. In the latter procedure, on the other hand, the growth rate is as high as around 0.1Å/mAmin even when the total pressure and partial pressures of diethylzinc and diethyltelluride were kept at 5×10^{-5}, 3×10^{-6} and 2×10^{-6} Torr, respectively (fig. 3). We have also carried out the growth experiment using the sapphire window. However, it has been found that no growth happens in this case, indicating that the photons corresponding to wavelengths below 1500Å is effective for the growth of ZnTe.

The authors would like to thank to Dr. Hiraya of UVSOR facility for his helpful discussion with the design of differential pumping system.

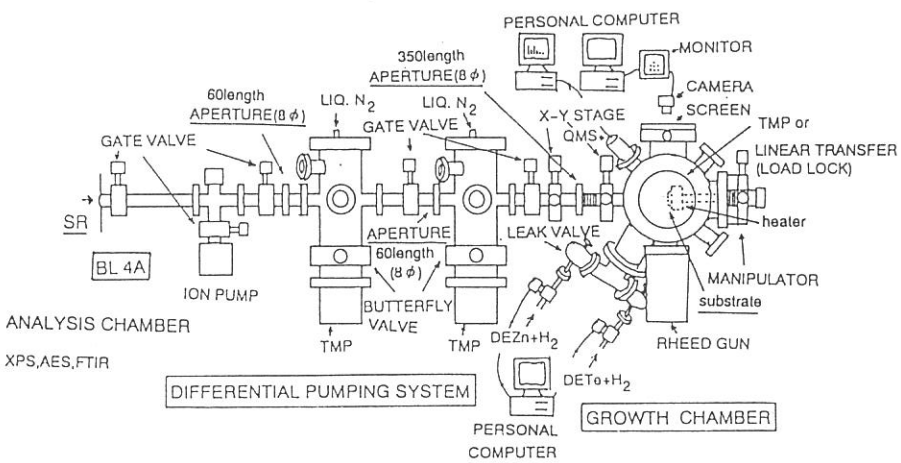

Fig.1. Schematical experimental apparatus.

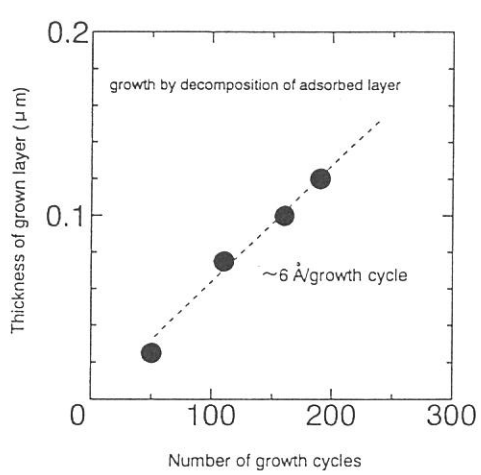

Fig.2. The thickness of the film versus the number of growth cycles.

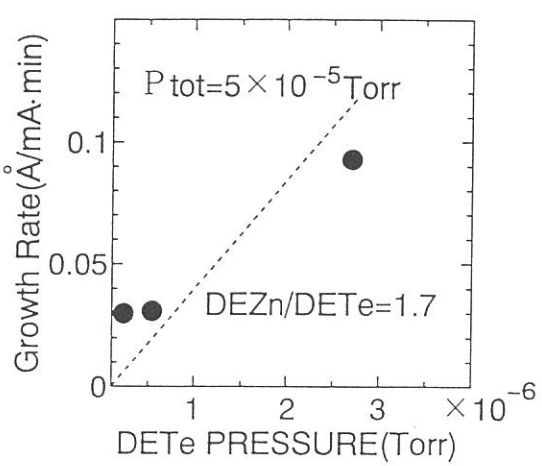

Fig.3. The growth rate of the film versus the partial pressure of diethyltelluride.

Construction of Infrared Reflection Absorption Spectroscopy for Study of Surface Photochemical Reactions Induced by Synchrotron Radiation

Mitsuru NAGASONO, Akitaka YOSHIGOE, Kazuhiko MASE, and Tsuneo URISU

Department of Vacuum UV Photoscience, Institute for Molecular Science, Myodaiji, Okazaki 444

Recently, surface photochemical reactions induced by synchrotron radiation (SR) have been applied to semiconductor processes such as atomic layer epitaxial growth and atomic layer etching. The reactions have different characters from thermal or plasma ones, but the detailed mechanism is scarcely explored.

The aim of the present study is to measure the change of the adsorbed species and/or the adsorption states under reactions induced by SR using infrared reflection absorption spectroscopy (IRAS), and to clarify the reaction mechanisms. Advantage of IRAS is high resolution as compared with electron energy loss spectroscopy, and feasibility to measure under presence of gas in a reaction chamber, i.e., *in situ*. This paper describes construction of IRAS for study of reactions induced by SR.

Fig. 1 shows the apparatus attached with an IRAS system. The apparatus consists of four ultra high vacuum chambers, i.e., an etching, an epitaxial growth, a sample storage, and an airlock chamber. The IRAS system is composed of a Fourier transform infrared spectrometer (FTIR: JEOL JIR-7000), three mirror systems and a mercury cadmium telluride (MCT) detector, and can measure the reactions in the etching and the epitaxial chamber. Optical paths are purged with dry air without CO_2. For measurements in the etching chamber, a collimated parallel infrared beam that is interfered by the FTIR is focused on the sample at an incident angle of 85° by an off-axis paraboloidal mirror M2 (diameter, D = 50mm, effective focal length, F = 320mm, diverting angle, α = 65°) through a ZnSe window. A reflected beam is collimated again by a mirror M5 (D = 50mm, F = 320, α = 65°), and is focused on the MCT detector by mirror M6 (D = 50mm, F = 45mm, α = 90°). For measurements in the epitaxial growth chamber, the IR beam is focused at incident angle of 82.5° by a mirror M4 (D = 50mm, F = 320, α = 90°) through a ZnSe window. The reflected beam is collimated by a mirror M7 (D = 50mm, F = 320, α = 90°), and is focused on the MCT detector by

mirror M8 (D = 50mm, F = 45mm, $\alpha = 90^{\circ}$). The signals from the MCT detector are amplified, and give IR spectra after fast FT calculation.

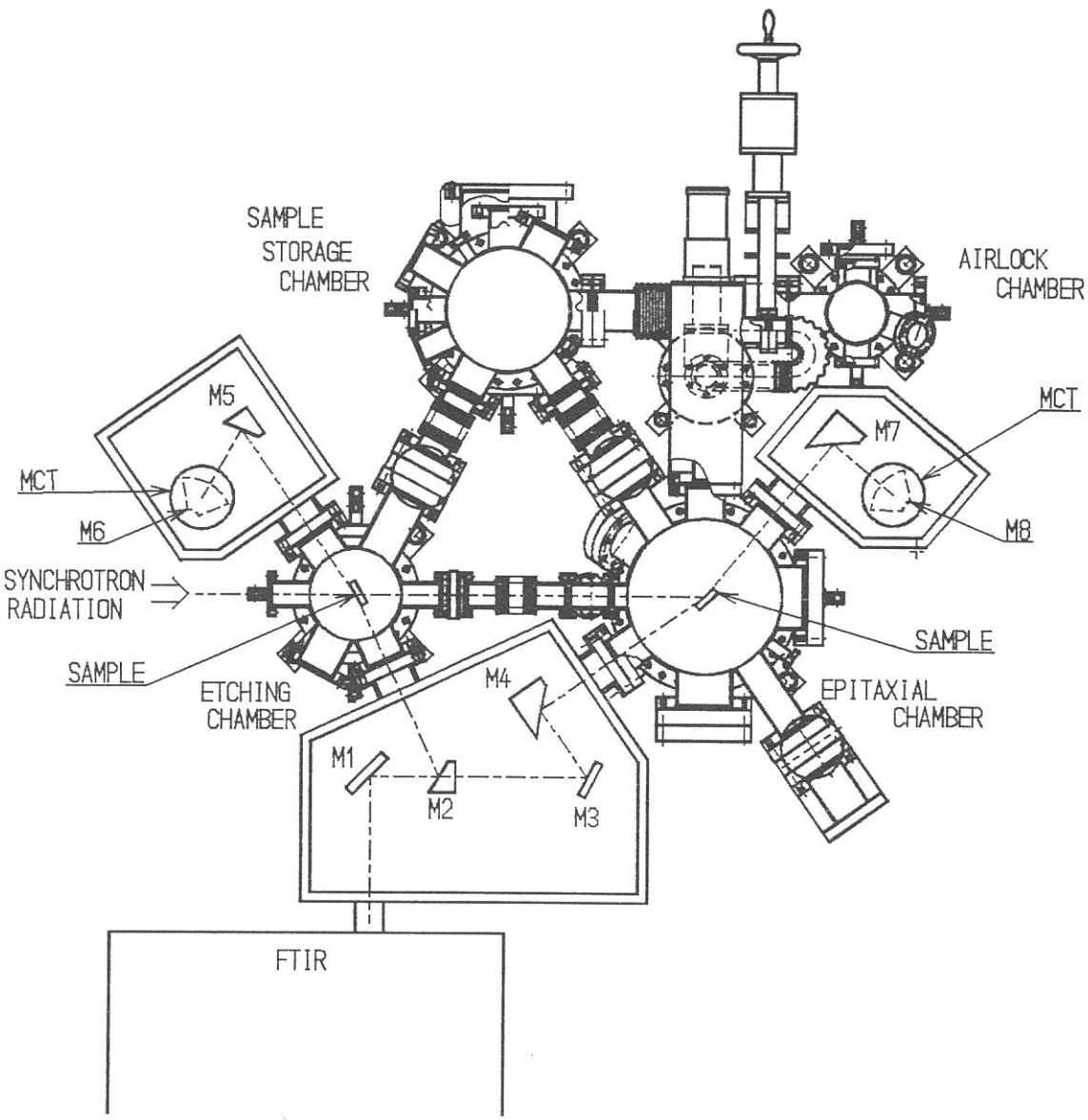

Fig. 1 IRAS system for study of SR excited surface photochemical reactions. For measurements in the etching chamber, IR beam passes through M1, M2, Sample, M5, and M6. For measurements in the epitaxial growth chamber, IR beam passes through M1, M3, M4, Sample, M7, and M8.